Phisically-based Dirac's deltas functions in the static analysis of multi-cracked Euler-Bernoulli and Timoshenko beams

Alessandro Palmeri[a,*], Alice Cicirello[b,1]

[a]*Department of Civil and Building Engineering, Loughborough University, Sir Frank Gibb Building, Loughborough LE11 3TU, UK*
[b]*School of Engineering, Design and Technology, University of Bradford, Richmond Road, Bradford BD7 1DP, UK*

Abstract

Dirac's delta functions enable simple and effective representations of point loads and singularities in a variety of structural problems, leading very often to elegant and otherwise unworkable closed-form solutions. This is the case of cracked beams under static loads, whose theoretical and practical significance has attracted in recent years the interest of many researchers. Nevertheless, analytical formulations currently available for this problem are not completely satisfactory, either in terms of computational efficiency, when the continuity conditions must be enforced with auxiliary equations, or in terms of physical consistency, when the singularities in the beam's flexural rigidity are represented with Dirac's delta functions having a questionable negative sign. These considerations motivate the present study, which offers a novel and physically-based modelling of slender Euler-Bernoulli beams and short Timoshenko beams with any number and severity of cracks, conducing in both cases to exact closed-form solutions. For validation purposes in non-trivial examples, a standard finite element code is used, along with two nascent deltas (uniform and Gaussian density functions) to describe a smeared increase in the bending flexibility around the abscissa of the crack.

Keywords: Concentrated crack, Dirac's delta function, Theory of distributions, Euler-Bernoulli beam, Timoshenko beam, Generalized functions

1. Introduction

Structural analysis of multi-cracked beams is of great engineering interest, and has been extensively studied in the last decades. As a matter of fact, presence of cracks may radically change the behaviour of beams and reduce their performances in statics and dynamics, leading to excessive deflections and unexpected failures.

Research in this field has been mainly concentrated on two classes of problems: *i*) definition of appropriate linear and non-linear models for representing the effects of cracks under static and dynamic loadings and *ii*) detection of position and severity of the damage by using either static or dynamic tests (e.g., Banan and Hjelmstad, 1994; Dimarogonas, 1996; Hjelmstad and Shin, 1997; Chondros et al., 1998). Belonging to the first stream of research, this paper deals with an effective and physically-based linear modelling of multi-cracked beams subjected to static loadings, although the results presented herein can be useful for treating any type of concentrated damage occurring in slender and short beams, e.g. corrosion of steel bars in reinforced concrete members, defects of material and attacks of biotic agents in timber elements, and etcetera. Indeed, the proposed model enables one to analytically represent a local increase in the bending flexibility of the beam, which is actually what all the types of damage mentioned above have in common. According to the classification by Friswell and Penny (2002), the proposed approach falls in the broad category of "discrete spring models", being equivalent to an internal hinge coupled with a linear elastic spring, which is herein assumed to have constant rigidity independently of the loading direction. Although very simple, this "always open" model (Irwin, 1957) proves to be very efficient for static problems (Buda and Caddemi, 2007; Caddemi and Morassi, 2007; Caddemi and Di Paola, 2008); it can be also applied to dynamic problems when the amplitude of vibration is smaller than the static deflection (Chondros et al., 2001), while "breathing in time" models (Kirmsher, 1944) are mandatory when cracks open and close, in so causing more complicated nonlinear phenomena. Extended finite element method (e.g. Belytschko and Black, 1999; Moës et al., 1999) and meshless methods (e.g. Nguyen et al., 2008; Yaw et al., 2009) are very powerful computational strategy in this context, particularly when initiation and propagation of cracks are studied in 2D or 3D models of structural members.

Classical analytical approaches are particular appealing when the global behaviour of frame structures is concerned. The idea of treating multi-cracked beams with equivalent linear springs at the cracks' position is based on the partition of the each member into undamaged pieces between two consecutive cracks. For slender Euler-Bernoulli beams, the governing fourth-order differential equation of bending can be written for each subsystem, but it is necessary to impose the pertinent continuity conditions between adjacent subsystems to obtain the

*Corresponding author
Email addresses: A.Palmeri@lboro.ac.uk (Alessandro Palmeri), ac685@cam.ac.uk (Alice Cicirello)
[1]Currently with: Department of Engineering, University of Cambridge, Trumpington Street, Cambridge CB2 1PZ, UK.

static response of the whole beam. As a results, the computational effort increases with the number of cracks: that is, for n cracks along the beam, $4(n+1)$ algebraic equations have to be solved to compute the $4(n+1)$ integration constants. Clearly, this way to proceed is computationally inefficient and is not particularly convenient for identifications purposes, when analyses are repeated until position and severity of the damage are found.

Moving from the same idea, a FEM (finite element method) approach has been recently pursued (Skrinar and Pliberšek, 2007; Skrinar, 2009), in which stiffness matrix and load vector of the uncracked Euler-Bernoulli beam are modified with some dimensionless coefficients which take into account the effects of internal cracks. These coefficient have to be evaluated, for each cracked member, by exploiting the continuity equations between adjacent uncracked segments.

A completely different strategy is to make use of the so-called generalized functions to handle static and kinematical discontinuities along the beam (Macaulay, 1919; Brungraber, 1965). Among others, Yavari et al. (2000) used the auxiliary beam method to solve the governing equations for uniform Euler-Bernoulli and Timoshenko beams with various jump discontinuities; Yavari et al. (2001) derived the differential equations in terms of single displacement and rotation functions for non-uniform beams with transverse and rotation jumps. These procedures, however, do require the enforcements of continuity conditions at each jump, and hence additional integration constants are needed. This issue has been tackled in the formulation originally developed by Biondi and Caddemi (2005, 2007), which will be referred in what follows as "rigidity modelling". This basically consists of singularities in the flexural stiffness represented by Dirac's delta functions, which in turn are equivalent to internal hinges with rotational linear-elastic springs. For uniform slender beams under static transverse load, this approach enables one to compute the exact deflection in closed form, and has been also used for a range of further structural problems, including theoretical buckling and modal analyses of multi-cracked Euler-Bernoulli members (Caddemi and Calió, 2008, 2009), and experimental static (Buda and Caddemi, 2007) and dynamic (Caddemi et al., 2010) investigations.

Even though computationally very efficient, and able to deliver elegant closed-form (exact) solutions, this rigidity modelling lacks physical consistency. The reason is that, as stressed by Buda and Caddemi (2007), the bending stiffness of the cracked beam is represented in their approach by a distribution, rather than by a classical function. As a consequence, from a mere mathematical point of view, it is only required the integrability of the bending stiffness for a suitable choice of test functions (e.g., Strichartz, 2003). From a more physical perspective, however, when Dirac's delta functions are substituted with proper nascent deltas (e.g., Kelly, 2006), it would be expected that meaningless negative signs do not appear in the flexural rigidity of the cracked beam. Unfortunately, the opposite happens with the analytical solutions by Caddemi and his associates, which then result to be not completely satisfactory. Moreover, this approach has been suggested to be unable of tackling mixed-type singularities in Euler-Bernoulli beams, i.e. slender beams where discontinuities in terms of rotation and bending moment occur at the same location (Failla and Santini, 2007). Finally to the best of authors' knowledge, the extension of rigidity modelling via Dirac's delta functions to cope with multi-cracked short Timoshenko beam is not available in the literature.

Aimed at addressing the above issues, an alternative and physically-based "flexibility modelling" of concentrated damages is presented in this paper, leading to exact solutions for the static analysis of multi-cracked Euler-Bernoulli beams in bending, which are fully equivalent to those obtained with the rigidity modelling (Biondi and Caddemi, 2007). Comparison with two nascent deltas, selected as uniform and Gaussian probability density functions, demonstrate the physical soundness of the proposed approach, while the rigidity modelling cannot be used in conjunction with nascent deltas, as a negative stiffness would appear. It will be also shown that the exact solutions catered by both rigidity and flexibility modelling can be applied to every mixed type of internal and external discontinuities provided that proper representations are used for the generalised functions. Finally, the proposed approach will be extended to take into account shear deformations in the undamaged pieces of a short member, which allow deriving exact solutions for the static analysis of multi-cracked Timoshenko beams.

2. Bending deflection of inhomogeneous Euler-Bernoulli elastic beams

Aim of this section is to review the differential equation governing the bending deflection of inhomogeneous Euler-Bernoulli beams. These equations will be particularised in the next section either with concentrated losses of rigidity or concentrated increases in the flexural flexibility of the beam, i.e. with two alternative inhomogeneous terms for modelling the macroscopic effects of cracks and similar localized damages.

Let us consider an elastic slender beam with abscissa-dependent flexural stiffness $E(z)I(z)$, where $E(z)$ and $I(z)$ are Young's modulus and second moment of area, respectively, while z is the spatial coordinate spanning from 0 to the length l of the member. Within the Euler-Bernoulli beam's theory, equilibrium Eqs. (1), compatibility Eqs. (2) and constitutive Eq. (3) read:

$$\frac{\mathrm{d}}{\mathrm{d}z}V(z)+q(z)=0; \qquad \frac{\mathrm{d}}{\mathrm{d}z}M(z)-V(z)=0; \tag{1}$$

$$\chi(z)=\frac{\mathrm{d}}{\mathrm{d}z}\varphi(z); \qquad \varphi(z)=-\frac{\mathrm{d}}{\mathrm{d}z}u(z); \tag{2}$$

$$\chi(z)=\frac{M(z)}{E(z)I(z)}, \tag{3}$$

where $M(z)$ and $V(z)$ are bending moment (positive if sagging) and shear force along the beam; $u(z)$, $\varphi(z)$ and $\chi(z)$ are deflection (positive if downward), slope and curvature functions, respectively; $q(z)$ is the transverse load on the beam (positive if downward). Combining the Eqs. (1) to (3) yields to the well-known Euler-Bernoulli fourth-order differential equation for beams in bending:

$$\frac{\mathrm{d}^2}{\mathrm{d}z^2}\left[E(z)I(z)\frac{\mathrm{d}^2}{\mathrm{d}z^2}u(z)\right]=q(z). \tag{4}$$

For the subsequent developments, it is more convenient to work with the dimensionless counterpart of Eq. (4):

$$\left[\widetilde{EI}(\zeta)\widetilde{u}''(\zeta)\right]'' = \widetilde{q}(\zeta), \tag{5}$$

where the prime denotes differentiation with respect to the dimensionless abscissa $\zeta = z/l$, which takes values from 0 to 1, and:

$$\widetilde{u}(\zeta) = \frac{u(\zeta\, l)}{l}; \qquad \widetilde{q}(\zeta) = \frac{q(\zeta\, l)\, l^3}{EI_0}; \qquad \widetilde{EI}(\zeta) = \frac{E(\zeta\, l)\, I(\zeta\, l)}{EI_0}, \tag{6}$$

EI_0 being the reference value of the flexural stiffness, e.g. the uncracked value of a significant cross section, while the overtilde denotes dimensionless functions of ζ.

3. Rigidity versus flexibility modelling of cracks with Dirac's delta functions

Two alternative formulations for modelling concentrated cracks via Dirac's delta functions are compared in this section. The first approach has been successfully used in recent years by Caddemi and his associates (Biondi and Caddemi, 2005, 2007; Buda and Caddemi, 2007; Caddemi and Calió, 2008, 2009) in a variety of structural problems involving cracked slender members. In these papers, a Dirac's delta function with negative sign accounts for the concentrated loss of flexural stiffness at the crack's position. The novel model proposed in this paper consists of a Dirac's delta function with positive sign in the flexural flexibility. Both models lead to exact (and thus equivalent) closed-form solutions for the differential equations of multi-cracked slender beams in bending, which are presented and discussed. The problem is illustrated in Fig. 1, in which a slender beam cracked at the abscissa $z = \bar{z}_j$ and subjected to the generic transverse load $q(z)$ is shown (left), along with the corresponding macroscopic model with a rational spring of stiffness K_j (right).

3.1. Rigidity modelling reviewed

Originally proposed by Biondi and Caddemi (2005), the modelling of cracks via Dirac's delta functions as loss of rigidity leads to the following expression of the dimensionless flexural stiffness of the beam:

$$\widetilde{EI}(\zeta) = 1 - \sum_{j=1}^{n} \beta_j \delta(\zeta - \bar{\zeta}_j), \tag{7}$$

where n is the number of concentrated cracks, $\bar{\zeta}_j = \bar{\zeta}_j/l$ is the dimensionless abscissa where the $j-th$ crack occurs, and the parameter β_j is related to the dimensionless stiffness of the corresponding rotational spring:

$$\widetilde{K}_j = \frac{K_j\, l}{EI_0} = \frac{1 - \beta_j \widetilde{A}}{\beta_j}, \tag{8}$$

where K_j is the actual value of the stiffness and $\widetilde{A} = 2.013$ is a positive constant which has been suggested by Bagarello (1995) for representing the product of two Dirac's deltas both centred at the same point $\bar{\zeta}$:

$$\delta(\zeta - \bar{\zeta})\, \delta(\zeta - \bar{\zeta}) = \widetilde{A}\, \delta(\zeta - \bar{\zeta}). \tag{9}$$

It is worth noting that, according to Eq. (8), the parameter β_j is subjected to the constrain $0 \le \beta_j \le 1/\widetilde{A}$ in order to avoid a negative value for the stiffness K_j. Substituting Eq. (7) into Eq. (5), after some algebra and resorting to the properties of Dirac's delta functions, the following exact solution in terms of deflection for multi-cracked Euler-Bernoulli beams has been proposed in closed-form (Biondi and Caddemi, 2007):

$$\begin{aligned}\widetilde{u}(\zeta) = C_1 + C_2\zeta + C_3\left[\zeta^2 + 2\sum_{j=1}^{n} \widetilde{K}_j^{-1}\left(\zeta - \bar{\zeta}_j\right) H(\zeta - \bar{\zeta}_j)\right] \\ + C_4\left[\zeta^3 + 6\sum_{j=1}^{n} \widetilde{K}_j^{-1}\,\bar{\zeta}_j\left(\zeta - \bar{\zeta}_j\right) H(\zeta - \bar{\zeta}_j)\right] \\ + \widetilde{q}^{[4]}(\zeta) + \sum_{j=1}^{n} \widetilde{K}_j^{-1}\,\widetilde{q}^{[2]}(\bar{\zeta}_j)\left(\zeta - \bar{\zeta}_j\right) H(\zeta - \bar{\zeta}_j),\end{aligned} \tag{10}$$

where $\widetilde{q}^{[m]}(\zeta)$ stands for the primitive of order m of the loading function $\widetilde{q}(\zeta)$, and $H(\zeta)$ indicates the Heaviside's unit step function, which in turn is the primitive of the Dirac's delta function centered at zero:

$$H(\zeta) = \delta^{[1]}(\xi) = \int_{-\infty}^{\zeta} \delta(\xi)\mathrm{d}\xi = \begin{cases} 0, & \zeta < 0; \\ \frac{1}{2}, & \zeta = 0; \\ 1, & \zeta > 0. \end{cases} \tag{11}$$

Interested readers can find the full mathematical derivation of Eq. (10) in the paper by Biondi and Caddemi (2007).

Moreover, it is worth noting that alternative definitions of the Heaviside's unit step function are known to the literature (e.g., Muscolino and Palmeri, 2005), which differ in the value of $H(\zeta)$ at $\zeta = 0$ (either $H(0) = 0$ or $H(0) = 1$) and may have a huge impact on the modelling of engineering systems and phenomena. Even though Biondi and Caddemi (2005, 2007) do not explicitly define the value of the unit step at the origin, it seems sensible in the present context to assume $H(0) = \frac{1}{2}$. Indeed, this choice is consistent with a symmetric distribution of the loss of rigidity with respect to the generic abscissa $\bar{\zeta}_j$, which is what is actually expected (unless further information on the crack is available). From a mere mathematical point of view, the value $H(0)$ is not strictly required in the vast majority of the situations, in which it provides a clear link between mathematical modelling and engineering intuition of the problem. However, when a concentrated couple is applied at the same position of a cracked section (i.e. the limitation suggested by Failla and Santini (2007)), the value of the Heaviside's unit step function at the discontinuity turns out to be very important, as shown in the first numerical application (Section 6.1).

3.2. Proposed flexibility modelling

Although leading to an exact solution for the problem in hand, the mathematical modelling of concentrated cracks with Dirac's

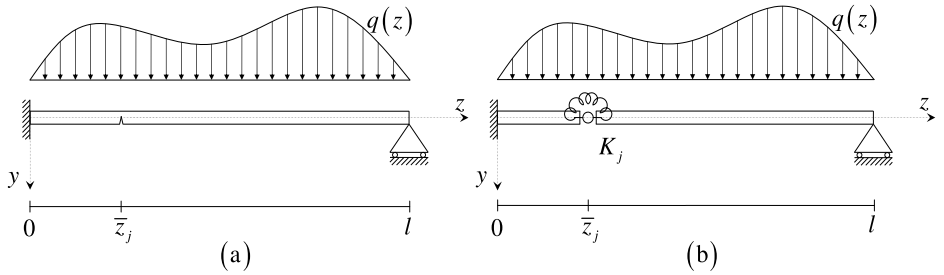

Figure 1: Sketches of cracked beam (a) and corresponding linear-elastic macroscopic model (b).

deltas in the flexural stiffness of the beam is not physically consistent. Indeed, it is well known that a Dirac's delta can be used to represent lumped quantities in the domain of definition, where impulsive singularity appears. Hence, according to Eq. (7), the application of a Dirac's delta at the position of the $j-th$ crack, $\zeta = \bar{\zeta}_j$, results in a negative impulse in the flexural stiffness. Fig. 2 (a) makes use of the same representation adopted by Biondi and Caddemi (2005, 2007) to illustrate the concept of a concentrated loss of rigidity at the position of the crack. This picture clearly highlights the physical inconsistency of the rigidity modelling, in which the flexural stiffness $EI(z)$ ideally goes to $-\infty$ at the cracked sections $z = \bar{z}_j$. It can be argued that the value of a Dirac's deltas is not defined strictly where the singularity occurs, but there is still a negative flexural stiffness somehow lumped at the position of the crack. It could be quite challenging to explain this concept in simple terms (e.g. in an undergraduate module of Structural Analysis), since the rigidity modelling so formulated and represented seems to violate the principle that elastic rigidities are always non-negative. To overcome this apparent flaw, Dirac's deltas centered at the position of the cracks are used as test functions in the mathematical derivations proposed by Biondi and Caddemi (2005, 2007), recalling also the properties of the product of the two Dirac's deltas at the same abscissa (Bagarello, 1995), which in turn leads to the parameter $\widetilde{A}$ appearing in Eq. (8).

Aimed at overcoming the misleading representation of negative impulses in the flexural stiffness (Fig. 2(a)), and avoiding unnecessary involved mathematical concepts (including the seemingly arbitrary parameter $\widetilde{A}$, which actually does not appear in the final expression (Eq. (10)), it seems more appropriate to introduce Dirac's deltas in the bending flexibility:

$$\widetilde{EI}(\zeta)^{-1} = 1 + \sum_{j=1}^{n} \alpha_j \, \delta(\zeta - \bar{\zeta}_j) \,, \tag{12}$$

where the dimensionless parameter α_j defines the intensity of the $j-th$ impulse, which in fact is related to the severity of the damage at $\zeta = \bar{\zeta}_j$, i.e. the larger is α_j, the more severe is the $j-th$ damage. Fig. 2(b) shows a graphical representation of the proposed flexibility modelling, where Dirac's deltas are associated to lumped increases in flexural flexibility.

Upon substitution of Eq. (12) into Eq. (5), one obtains:

$$\left\{ \left[1 + \sum_{j=1}^{n} \alpha_j \, \delta(\zeta - \bar{\zeta}_j) \right]^{-1} \widetilde{u}''(\zeta) \right\}'' = \widetilde{q}(\zeta) \,, \tag{13}$$

whose double integration leads to:

$$\widetilde{u}''(\zeta) = \left[1 + \sum_{j=1}^{n} \alpha_j \, \delta(\zeta - \bar{\zeta}_j) \right] \left(\widetilde{q}^{[2]}(\zeta) + C_1 \zeta + C_2 \right) , \tag{14}$$

where C_1 and C_2 are two unknown integration constants. Taking the Laplace's transform of both sides of Eq. (14) yields:

$$\widetilde{U}(s) = \mathscr{L}\langle \widetilde{u}(\zeta) \rangle = \frac{1}{s^2} \left[\frac{C_1}{s^2} + \frac{C_2}{s} + C_3 + C_4 s + \mathscr{L}\langle \widetilde{q}^{[2]}(\zeta) \rangle + \sum_{j=1}^{n} \alpha_j e^{-\bar{\zeta}_j s} \left(C_1 \bar{\zeta}_j + C_2 + \widetilde{q}^{[2]}\left(\bar{\zeta}_j\right) \right) \right] ; \tag{15}$$

where $\mathscr{L}\langle \bullet \rangle$ stands for the Laplace's transform operator, while s is the Laplace's variable associated with the dimensionless abscissa ζ. Taking now the inverse Laplace's transform, we get:

$$\widetilde{u}(\zeta) = \mathscr{L}^{-1}\langle \widetilde{U}(s) \rangle = C_4 + C_3 \zeta + \frac{1}{2} C_2 \zeta^2 + \frac{1}{6} C_1 \zeta^3 + \widetilde{q}^{[4]}(\zeta) + \sum_{j=1}^{n} \alpha_j \left(\zeta - \bar{\zeta}_j \right) H(\zeta - \bar{\zeta}_j) \left[C_2 + C_1 \bar{\zeta}_j + \widetilde{q}^{[2]}(\bar{\zeta}_j) \right] . \tag{16}$$

It is worth emphasizing that, similarly to Eq. (10) for the rigidity modelling, the beam's deflection of Eq. (16), obtained with the proposed flexibility modelling, depends on four integration constants only (C_1, C_2, C_3 and C_4), and that these quantities can be evaluated by means of boundary conditions only, without the enforcement of continuity conditions where the singularities are located. Moreover since Eq. (10) and Eq. (16) are two closed-form solutions of the same boundary-value elastic problem, they are equivalent, although the proposed derivation just involves very popular mathematical tools, namely Laplace's transform (Eq. (15)) and inverse Laplace's transform (Eq. (16)).

The first derivate of Eq. (16) gives the slope function:

$$\varphi(\zeta) = -\widetilde{u}'(\zeta) = -C_3 - C_2 \zeta - \frac{1}{2} C_1 \zeta^2 - \widetilde{q}^{[3]}(\zeta) - \sum_{j=1}^{n} \alpha_j H(\zeta - \bar{\zeta}_j) \left[C_2 + C_1 \bar{\zeta}_j + \widetilde{q}^{[2]}(\bar{\zeta}_j) \right] . \tag{17}$$

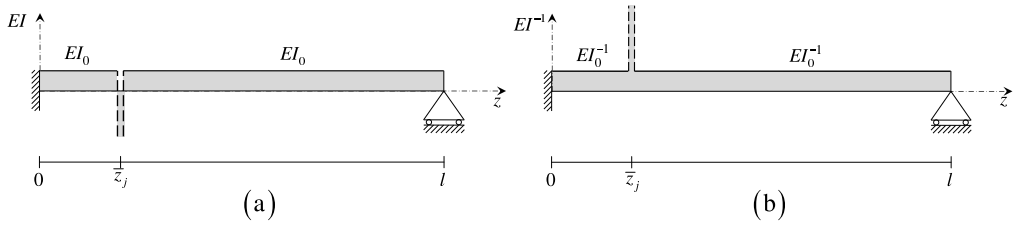

Figure 2: Negative Dirac's delta in the rigidity modelling of cracked beam (a), and positive counterpart in the flexibility modelling (b).

It follows that the jump discontinuity in the slope function, $\Delta\varphi_j$, that occurs at the position of the $j-th$ crack, $\bar{\zeta}_j$, takes the expression:

$$\Delta\varphi_j = \lim_{\zeta\to\bar{\zeta}_j^+}\varphi(\zeta) - \lim_{\zeta\to\bar{\zeta}_j^-}\varphi(\zeta) = -\alpha_j\left[C_2 + C_1\bar{\zeta}_j + \widetilde{q}^{[2]}(\bar{\zeta}_j)\right], \quad (18)$$

where the continuity of $q^{[2]}(\zeta)$ has been assumed at $\zeta = \bar{\zeta}_j$ (this condition is met even for point load $q(\zeta) \propto \delta(\zeta - \bar{\zeta}_j)$ and concentrated couple $q(\zeta) \propto \delta'(\zeta - \bar{\zeta}_j)$).

Dimensionless bending moment $\widetilde{M}(\zeta)$ and shear force $\widetilde{V}(\zeta)$ can be also obtained by considering first and second derivatives of Eq. (17), respectively:

$$\widetilde{M}(\zeta) = \frac{M(\zeta\, l)\, l}{EI_0} = -\widetilde{EI}(\zeta)\widetilde{u}''(\zeta) = -C_2 - C_1\,\zeta - \widetilde{q}^{[2]}(\zeta); \quad (19)$$

$$\widetilde{V}(\zeta) = \frac{V(\zeta\, l)\, l^2}{EI_0} = -\widetilde{EI}(\zeta)\widetilde{u}'''(\zeta) = -C_1 - \widetilde{q}^{[1]}(\zeta), \quad (20)$$

where the singularities arising from the summation in the right-hand side of Eq. (17) are compensated by those in flexural flexibility of Eq. (12). Comparing now Eqs. (18) and (19) leads to:

$$\Delta\varphi_j = \alpha_j\frac{\widetilde{M}\left(\bar{\zeta}_j\, l\right) l}{EI_0}. \quad (21)$$

At the macroscopic level, on the other hand, jump in the rotation, $\Delta\varphi_j$, and bending moment at the position of the $j-th$ crack, $M\left(\bar{\zeta}_j\, l\right)$, are related by:

$$\Delta\varphi_j = \frac{\widetilde{M}\left(\bar{\zeta}_j\, l\right)}{K_j}. \quad (22)$$

Equating now the right-hand side of Eqs. (21) and (22), one gets:

$$\alpha_j = \frac{EI_0}{K_j\, l} = \frac{1}{\widetilde{K}_j}, \quad (23)$$

which defines the mathematical relationship between the flexibility parameter α_j and the elastic stiffness of the rotational spring of the corresponding internal hinge K_j.

Interestingly, the coefficient α_j can be viewed ad a measure of the severity of the $j-th$ concentrated damage: at the limiting condition when $\widetilde{K}_j \to 0$, i.e. with an internal hinge with no rotational stiffness, α_j goes to infinity, which means that the cross section is fully damaged, and hence does not provide any flexural rigidity; on the contrary, for $\widetilde{K}_j \to +\infty$, i.e. without solution of continuity in the beam's flexibility, $\alpha_j \to 0$, which is the case of an undamaged cross section.

4. Flexibility modelling by means of two nascent deltas

In the previous section, two alternative representations of concentrated cracks in slender beams through Dirac's delta functions have been compared. The proposed mathematical derivation is straightforward, as it simply involves Laplace's transform and inverse Laplace's transform (Section 3.2). It has been also argued that the proposed flexibility modelling is preferable, in so avoiding the questionable negative impulses appearing in the rigidity modelling (Section 3.1) by Caddemi and his associates.

Aimed at proving the argument, the Dirac's delta function $\delta(\zeta)$ in the flexibility modelling (Eq. (12)) will be treated in this section as the ideal limit of two alternative sequences of nascent deltas, i.e. approximating impulse functions.

As usual in the context of probability theory, a nascent delta is herein an even Probability Density Function (PDF) with zero mean and dispersion around the centre going to zero. Without lack of generality, uniform (Section 4.1) and Gaussian (Section 4.2) PDFs will be considered to model the smeared increase in the bending flexibility at the position of cracks. It could be worth emphasizing that PDFs are used in our formulation to describe a deterministic increment in the beam's bending flexibility in the vicinity of each crack, rather than a random fluctuation of this quantity.

4.1. Uniform PDF

Let $\delta_{\tilde{p}}^{(\mathrm{U})}(\zeta)$ be the PDF of a dimensionless zero-mean random variable uniformly distributed in the interval $[-\tilde{p}, \tilde{p}]$, which can be mathematically defined as:

$$\delta_{\tilde{p}}^{(\mathrm{U})}(\zeta) = \frac{1}{2\,\tilde{p}}[H(\zeta + \tilde{p}) - H(\zeta - \tilde{p})]. \quad (24)$$

The PDF $\delta_{\tilde{p}}^{(\mathrm{U})}(\zeta)$ is a nascent delta, since the Dirac's delta can be obtained as the dispersion parameter $\tilde{p}$ goes to zero:

$$\delta(\zeta) = \lim_{\tilde{p}\to 0^+}\delta_{\tilde{p}}^{(\mathrm{U})}(\zeta), \quad (25)$$

as illustrated in Fig. 3(a).
Substitution of Eq. (24) into Eq. (12) gives the beam's bending flexibility in presence of n uniformly smeared cracks:

$$\widetilde{EI}(\zeta)^{-1} = 1 + \sum_{j=1}^{n}\alpha_j\,\delta_{\tilde{p}}^{(\mathrm{U})}(\zeta - \bar{\zeta}_j). \quad (26)$$

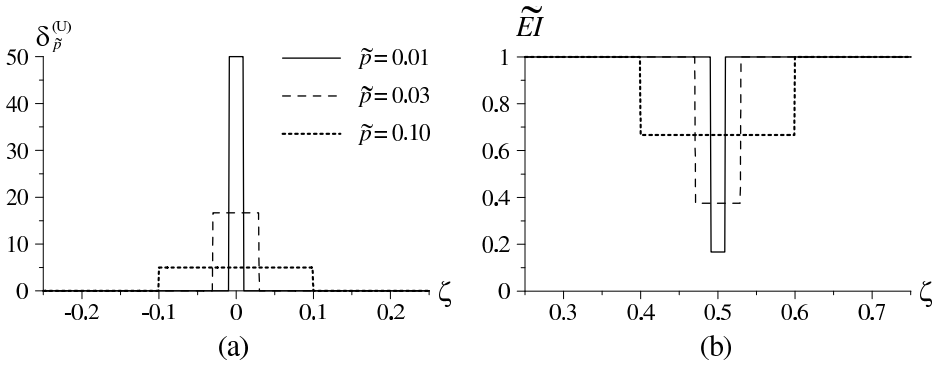

Figure 3: Nascent deltas as uniform PDF (a) and corresponding bending stiffness in the proposed flexibility modelling (b) for different values of the dispersion parameter $\tilde{p}$.

Incidentally, this model is equivalent to the representation of damage in slender beams proposed in the paper by Cerri and Vestroni (2000).

Assuming no overlapping cracked intervals, it follows that the dimensionless bending flexibility is: 1 outside the cracked areas of the beam; $1+\alpha_j/(2\,\tilde{p})$ within the interval $]\bar{\zeta}_j-\tilde{p},\bar{\zeta}_j+\tilde{p}[$. Hence, the corresponding flexural stiffness takes the dimensionless form:

$$\widetilde{EI}(\zeta)^{-1} = 1 - \sum_{i=1}^{2n} \gamma_i\, H(\zeta - \bar{\xi}_i)\,; \tag{27}$$

where intensity and location of the $j-th$ finite jump are given by:

$$\gamma_i = (-1)^i \Big/ \left(1 + \frac{2\,\tilde{p}}{\alpha_{\mathrm{int}[(1+i)/2]}}\right), \tag{28}$$

and:

$$\bar{\xi}_i = \bar{\zeta}_{\mathrm{int}[(1+i)/2]} + (-1)^i\,\tilde{p}\,, \tag{29}$$

respectively, int[•] being the integer part of the number within the square brackets.

It is worth noting that, according to Eq. (26), for the $j-th$ of the n smeared cracks there are two finite jumps in the dimensionless function $\widetilde{EI}(\zeta)$, namely a downward jump $\gamma_{2j-1} > 0$ at $\zeta = \bar{\xi}_{2j-1} = \bar{\zeta}_j - \tilde{p}$, which is recovered at $\zeta = \bar{\xi}_{2j} = \bar{\zeta}_j + \tilde{p}$ with an upward jump with the same module but opposite sign, $\gamma_{2j} = -\gamma_{2j-1} < 0$. As a results, $2n$ finite jumps appears in the right-hand side of Eq. (27).

For illustrative purpose, the bending stiffness $\widetilde{EI}(\zeta)$ is plotted in Fig. 3(b) in the neighborhood of a single smeared crack centered at $\bar{\zeta}_j = 0.5$ (beam's midspan), with different size parameters $\tilde{p}$ and intensity coefficient $\alpha_j = 0.1$.

With the adoption of the uniform PDF as nascent delta, the approximate model for the multi-cracked beam turns out to be a particular case of stepped beam, i.e. a beam with sudden changes in the flexural rigidity, which is constant between two consecutive jumps. The exact solution for the deformed shape of stepped beams under static transverse load has been obtained by Biondi and Caddemi (2007) in closed form:

$$\begin{aligned}\widetilde{u}(\zeta) = C_1 + C_2\,\zeta + C_3\Big[\zeta^2 + \sum_{i=1}^{2n} \gamma_i\,\mu_i\,\mu_{i+1}(\zeta-\bar{\xi}_i)^2 H(\zeta-\bar{\xi}_i)\Big)\Big] \\ + C_4\left[\zeta^3 + \sum_{i=1}^{2n} \gamma_i\,\mu_i\,\mu_{i+1}(\zeta^3 - 3\,\bar{\xi}_i^2\,\zeta + \bar{\xi}_i^3) H(\zeta-\bar{\xi}_i)\right] \\ + \overline{q}^{[4]}(\zeta) + \sum_{i=1}^{2n} \gamma_i\,\mu_i\,\mu_{i+1}\Big[\overline{q}^{[4]}(\zeta) - \overline{q}^{[4]}(\bar{\xi}_i) - (\zeta-\bar{\xi}_i)\,\overline{q}^{[3]}(\bar{\xi}_i)\Big] H(\zeta-\bar{\xi}_i)\,,\end{aligned} \tag{30}$$

in which:

$$\mu_i = \frac{1}{1 - \sum_{k=1}^{i-1} \gamma_k}; \tag{31}$$

once again, the four integration constants (C_1, C_2, C_3 and C_4) have to be evaluated by imposing the pertinent boundary conditions.

The general solution of Eq. (30) will be used in the next section to validate the proposed modelling of the bending flexibility with Dirac's delta functions (Section 3.2). Interested readers can find the mathematical derivation of Eq. (30) in the paper by Biondi and Caddemi (2007). A very similar expression has been independently derived by Cicirello (2007).

4.2. Gaussian PDF

As an alternative nascent delta, let us now consider the Gaussian PDF of a dimensionless random variable with zero mean and standard deviation $\tilde{\sigma} \ll 1$:

$$\delta^{(G)}_{\tilde{\sigma}}(\zeta) = \frac{1}{\sqrt{2\pi}\tilde{\sigma}} \exp\left[-\frac{1}{2}\left(\frac{\zeta}{\tilde{\sigma}}\right)^2\right]. \tag{32}$$

The dimensionless flexural rigidity with n cracks smeared with Gaussian law takes the expression:

$$\widetilde{EI}(\zeta) = \frac{1}{1 + \sum_{j=1}^{n} \alpha_j \delta^{(G)}_{\tilde{\sigma}}(\zeta - \bar{\zeta}_j)}\,. \tag{33}$$

The Gaussian PDF $\delta^{(G)}_{\tilde{\sigma}}(\zeta)$, being continuous, lends itself to approximate actual Dirac's delta functions in numerical analyses of problems with impulsive terms. As an example, this

nascent delta has been recently used to prove the existence of long-neglected impulsive forces occurring when a moving oscillator enters and exits the supporting beam (Muscolino et al., 2009).

For the sake of illustration, nascent Gaussian delta and corresponding flexural rigidity around a smeared crack with centre at $\zeta = \bar{\zeta}_j = 0.5$ and intensity coefficient $\alpha_j = 0.1$ are depicted in Fig. 4.

4.3. Rigidity modelling with nascent deltas

Figures 3(b) and 4(b) show that substitution of uniform and Gaussian nascent deltas into the proposed flexibility modelling (Eq. (12)) leads to meaningful flexural rigidities. The smaller is the dispersion parameters ($\tilde{p}$ and $\tilde{\sigma}$, respectively), the larger is the loss of stiffness at the abscissa of the crack, but always with a consistent positive value, which in turn demonstrates the physical soundness of the proposed model.

The opposite happens with the rigidity modelling by Caddemi and his associates. Indeed, by substituting the same approximate impulses of figures 3(a) and 4(a) into the bending stiffness of Eq. (7), one may obtain meaningless negative values in the neighborhood of the abscissa of the crack. Figures 5(a) and 5(b) show that just for large values of the dispersion parameter (i.e. $\tilde{p} = 0.1$ and $\tilde{\sigma} = 0.1$ for uniform and Gaussian PDFs, respectively) the resultant bending stiffness $\widetilde{EI}(\zeta)$ does not take negative values. When smaller values of the dispersion parameter are considered (dashed and solid lines in Fig. 5), instead of having a closer approximation of concentrated cracks (as it would be expected), the bending stiffness drops below zero, which is unacceptable from a physical point of view.

5. Multi-cracked short Timoshenko beams

In the previous part of the paper, Dirac's delta functions (Section 3.2) and nascent deltas (Sections 4.1 and 4.2) have been used to model concentrated and smeared cracks in slender Euler-Bernoulli beams. Aim of this section is to extend the proposed flexibility modelling of cracks through Dirac's deltas to cope with short Timoshenko beams. To do so, let us express the transverse deflection as superposition of bending ($\widetilde{u}_b(\zeta)$) and shearing ($\widetilde{u}_s(\zeta)$) contributions:

$$\widetilde{u}(\zeta) = \widetilde{u}_b(\zeta) + \widetilde{u}_s(\zeta)\,. \tag{34}$$

The first component, $\widetilde{u}_b(\zeta)$, is formally ruled by the same fourth-order differential equation considered for slender beams (Eq. (5)):

$$\left[\widetilde{EI}(\zeta)\widetilde{u}_b{}''(\zeta)\right]'' = \widetilde{q}(\zeta), \tag{35}$$

whose solution, in presence of n concentrated cracks, takes the same form as Eq. (16):

$$\widetilde{u}_b(\zeta) = C_4 + C_3\zeta + \frac{1}{2}C_2\,\zeta^2 + \frac{1}{6}C_1\,\zeta^3 + \overline{\overline{q}}^{[4]}(\zeta) + \sum_{j=1}^{n}\alpha_j\left(\zeta - \bar{\zeta}_j\right)H(\zeta - \bar{\zeta}_j)\left[C_2 + C_1\,\bar{\zeta}_j + \overline{\overline{q}}^{[2]}(\bar{\zeta}_j)\right]. \tag{36}$$

Moreover, rotation $\varphi(\zeta)$, bending moment $\widetilde{M}(\zeta)$ and shear force $\widetilde{V}(\zeta)$ are the same as in the Euler-Bernoulli beam (Eqs. (17), (19) and (20)), respectively:

$$\varphi(\zeta) = -\widetilde{u}'(\zeta) = -C_3 - C_2\,\zeta - \frac{1}{2}C_1\,\zeta^2 - \overline{\overline{q}}^{[3]}(\zeta) - \sum_{j=1}^{n}\alpha_j H(\zeta - \bar{\zeta}_j)\left[C_2 + C_1\bar{\zeta}_j + \overline{\overline{q}}^{[2]}(\bar{\zeta}_j)\right]; \tag{37}$$

$$\widetilde{M}(\zeta) = \frac{M(\zeta\,l)\,l}{EI_0} = -\widetilde{EI}(\zeta)\widetilde{u}''(\zeta) = -C_2 - C_1\,\zeta - \overline{\overline{q}}^{[2]}(\zeta); \tag{38}$$

$$\widetilde{V}(\zeta) = \frac{V(\zeta\,l)\,l^2}{EI_0} = -\widetilde{EI}(\zeta)\widetilde{u}'''(\zeta) = -C_1 - \overline{\overline{q}}^{[1]}(\zeta)\,. \tag{39}$$

The second component in the right-hand side of Eq. (34), $\widetilde{u}_s(\zeta)$, is ruled by:

$$\widetilde{GA}_s\widetilde{u}_s'(\zeta) = \widetilde{V}(\zeta), \tag{40}$$

where $\widetilde{GA}_s$ is the dimensionless shearing stiffness of the beam, which is assumed to be constant throughout the beam:

$$\widetilde{GA}_s = \frac{GA_0\,l^2}{EI_0\,\kappa}, \tag{41}$$

in which G is the shear modulus, A_0 is the uncracked cross-sectional area and κ is the so-called shear correction factor.

Substitution of Eq. (39) into Eq. (40) leads to:

$$\widetilde{u}_s'(\zeta) = -\widetilde{GA}_s{}^{-1}\left[C_1 + \overline{\overline{q}}^{[1]}(\zeta)\right], \tag{42}$$

By integrating once and assuming $\widetilde{u}_s(0) = 0$, without loss of generality, one obtains:

$$\widetilde{u}_s = -\widetilde{GA}_s{}^{-1}\left[C_1\zeta + \overline{\overline{q}}^{[2]}(\zeta)\right], \tag{43}$$

which represents the deflection of the beam due to pure shearing deformations. Substituting Eqs. (36) and (43) into Eq. (34) gives the dimensionless closed-form expression of transverse deflections in multi-cracked Timoshenko beams:

$$\widetilde{u}(\zeta) = C_4 + \left(C_3 - \widetilde{GA}_s{}^{-1}\right)\zeta + \frac{1}{2}C_2\,\zeta^2 + \frac{1}{6}C_1\,\zeta^3 + \overline{\overline{q}}^{[4]}(\zeta) - \widetilde{GA}_s{}^{-1}\overline{\overline{q}}^{[2]}(\zeta) + \sum_{j=1}^{n}\alpha_j\left(\zeta - \bar{\zeta}_j\right)H(\zeta - \bar{\zeta}_j)\left[C_2 + C_1\,\bar{\zeta}_j + \overline{\overline{q}}^{[2]}(\bar{\zeta}_j)\right]. \tag{44}$$

which depends once again on four integrations constants C_1, C_2, C_3 and C_4. The solution for Euler-Bernoulli beams (Eq. (16)) is recovered when the dimensionless shearing flexibility $\widetilde{GA}_s{}^{-1}$ goes to zero.

6. Numerical applications

Aim of this section is to validate the proposed flexibility approach by means of three numerical applications, which are also useful to highlights specific aspects of the formulation. In a first stage, a clamped-clamped slender beam with single

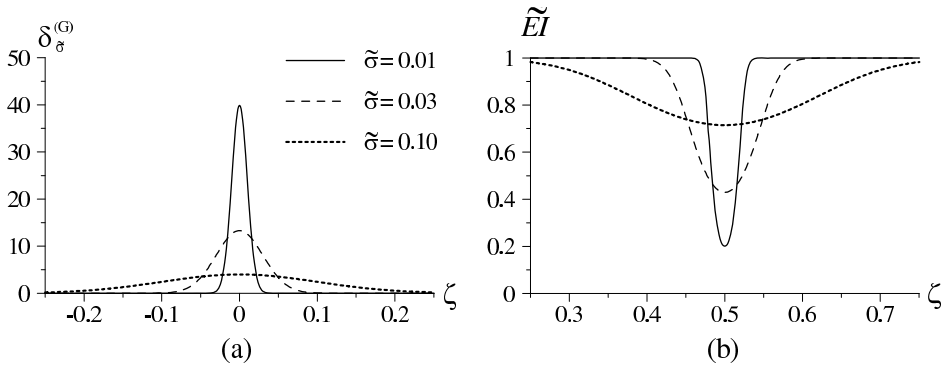

Figure 4: Nascent delta as Gaussian PDF (a) and corresponding bending stiffness in the proposed flexibility modelling (b) for different values of the standard deviation $\tilde{\sigma}$.

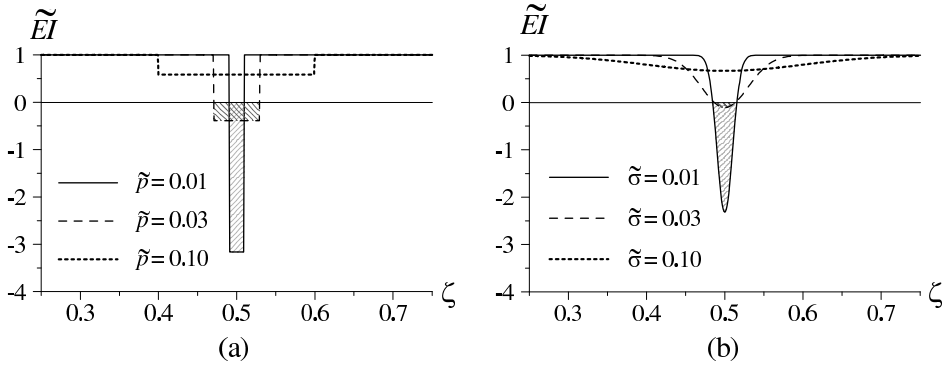

Figure 5: Bending stiffness when uniform (a) and Gaussian (b) nascent deltas are introduced in the rigidity modelling by Caddemi and his associates.

crack subjected to concentrated force and couple at the position of the damage has been studied (Section 6.1). This example has been suggested by the comment by Failla and Santini (2007) about a latent limitation of the rigidity modelling by Biondi and Caddemi (2005, 2007) when discontinuities of rotation and bending moment occur at the same location. It will be shown that a proper definition of the Heaviside's unit step function (see Eq. (11)) allows overcoming this limitation. In a second stage, a multi-supported multi-cracked Euler-Bernoulli beam has been considered (Section 6.2), in which the case of a crack located at one end of the beam has been addressed with the general solution of Eq. (16). To the best of authors' knowledge, numerical applications for this second type of problems are not available in the dedicated literature. In a third stage, the closed-form solution of Eq. (44) has been used for a short (Timoshenko) propped beam cracked at midspan. The results obtained with the proposed flexibility modelling have been compared with those of a standard FEM analysis carried out with the commercial software SAP2000 (version 14.1.0), and a perfect agreement has been observed in all three cases; the rigidity modelling by Biondi and Caddemi (2005, 2007) and the two nascent deltas, i.e. uniform and Gaussian PDFs, have been also considered for the first two slender beams.

In order to associate an appropriate value of the rotational spring stiffness K_j to the real depth of the $j-th$ crack, the expression suggested by Bilello (2001) for rectangular cross-sections has been used:

$$K_j = \frac{EI_0}{h}\,\frac{0.9[(d_j/h)-1]^2}{(d_j/h)\,[2-(d_j/h)]}\,, \tag{45}$$

where h and d_j are the depths of beam and crack, respectively. In both examples, the beam is assumed to be made of steel (Young's modulus $E = 210\,\text{GPa}$; $G = 80.77\,\text{GPa}$) and $l = 150\,\text{cm}$ long; In the first two cases (slender Euler-Bernolli beam) the cross section is a square of sides $h = b = 5\,\text{cm}$, while in the third case (short Timoshenko beam) the cross section is a rectangle $h = 45\,\text{cm}$ deep and $b = 15\,\text{cm}$ wide.

6.1. *Clamped-clamped slender beam subjected to concentrated force and couple*

In the first application (Fig. 6), a single crack of depth $d = 2.5\,\text{cm}$, is assumed at the abscissa $z = l/5 = 30\,\text{cm}$, where a concentrated couple $M = 20\,\text{kN m}$ and a point force $F = 70\,\text{kN}$

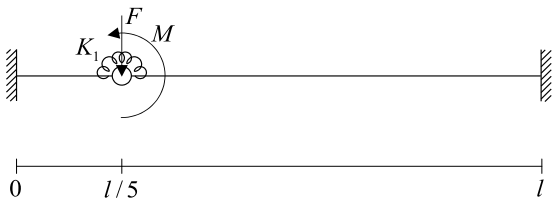

Figure 6: Sketch of the cracked slender beam considered in example 1.

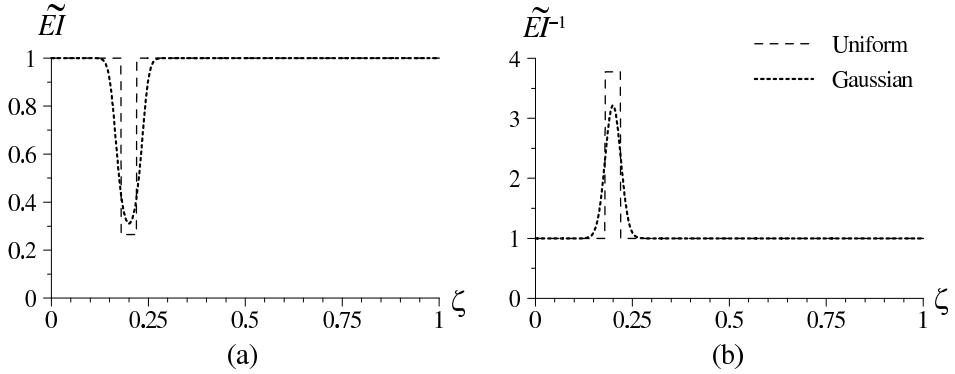

Figure 7: Bending flexibility (a) and rigidity (b) of the cracked beam of example 1 modelled with nascent deltas.

are also applied. Eq. (45) gives the value $K_1 = 656.25\,\mathrm{kN\,m}$ for the equivalent stiffness of the discrete spring at the position of the crack, while the dimensionless damage parameter of Eq. (23) is $\alpha_1 = 0.111$. Bending flexibility and rigidity along the beam are shown in the dimensionless Fig. 7(a) and Fig. 7(b), for uniform (dashed) and Gaussian (dotted) type of nascent delta, assuming dispersion parameters $\tilde{p} = 0.02$ and $\tilde{\sigma} = 0.02$, respectively; in both cases, inconsistent negative values do not appear.

The results in terms of deflection and rotation at the position of the crack are compared at the top of Tab. 1 for different methods of analysis. Interestingly, rigidity and flexibility modelling deliver the same exact results once the Heaviside's unit step function is defined as suggested in the right-hand side of Eq. (11), in so overcoming the limitation claimed by Failla and Santini (2007) for the applicability of the rigidity modelling when bending moment and slope are discontinuous at the same location. Rigidity and flexibility modelling are also in a very good agreement with the approximate solutions obtained by introducing nascent deltas in the bending flexibility, and with the FEM model built in SAP2000 with a rotational spring for the concentrated crack and two opposite forces with a small lever arm (2 cm) for the concentrated couple.

Fig. 8(a) and Fig. 8(b) show deformed shape and slope function of the beam, respectively. Rigidity and flexibility modelling match perfectly, since they give exact analytical solutions; displacements and rotations computed with nascent deltas compare also very well, although slightly larger deflections are predicted at the midspan of the beam. Dimensionless curvature $\widetilde{\chi}$ and bending moment $\widetilde{M}$ are offered in Fig. 9(a) and Fig. 9(b), respectively. As expected, the use of nascent deltas allow to graphically show the increased flexibility in the neighborhood of the crack, with two opposite peaks in the curvature (Fig. 9(a)), while Dirac's deltas concentrate this effect at the abscissa of the crack only, where a finite jump in the rotation occurs (Fig. 8(b)). The localised differences between modellings with nascent deltas (uniform and Gaussian) and Dirac's deltas (in terms of rigidity and flexibility) disappear in terms of bending moment (Fig. 9(b)), which virtually shows a perfect agreements among the four formulations. This is also confirmed by values of bending moment reported at the bottom of Tab. 1 for significant locations along the beam. It is worth emphasising here that, without a correct (i.e. physically-based) definition of the Heaviside function H, the analytical solutions derived with rigidity (Eq. (10)) and flexibility (Eq. (16)) modelling do not provide the correct results for the problem in hand. To prove the point, Fig. 10(a) shows the deflection $\widetilde{u}\left(\bar{\zeta}_1\right)$ at the position of the crack as a function of the dimensionless value θ assumed for the Heaviside function at zero, i.e. $H(0) = \theta$. In principle, θ can take any value from 0 to 1, and the picture demonstrates that this may have a significant impact on the results (i.e. the deflection at $\zeta = \bar{\zeta}_1$, may reverse sign). What is important to note is that rigidity modelling (circles) and flexibility modelling (solid line) are always in perfect agreement (i.e. these two closed-form solutions are equivalent), but the correct value of the deflection $\widetilde{u}\left(\bar{\zeta}_1\right)$ is obtained for $\theta = 0.5$ (as suggested in Eq. (11)). This is clearly demonstrated by comparison with the horizontal dashed line, which gives the exact value of $\widetilde{u}\left(\bar{\zeta}_1\right)$ as computed with the stiffness matrix method. Same considerations can be done looking at Fig. 10 (b), in which the finite jump $\Delta\varphi_1$ experienced by the beam at the position of the crack is plotted against the parameter θ: once again, $\theta = 0.5$ provides the correct results. As discussed above, taking the value $\theta = 0.5$ for $H(0)$ is fully consistent with the physical representation of the structural problem, although this aspect does not emerge very strongly from the rigidity modelling; the proposed flexibility modelling, on the contrary, has the additional merit to allow clarifying this point.

6.2. Multi-supported multi-cracked slender beam subjected to point load and support settlement

Similar trend of results can be observed for the second numerical example (Fig. 11), in which the same slender beam as in the previous application is restrained by a fixed support at the left-hand side end ($z = 0$) and by two roller supports at abscissas $z = 2l/5 = 60\,\mathrm{cm}$ and $z = 4l/5 = 120\,\mathrm{cm}$. The beam is subjected to a point force $F = EI_0/l^2 = 48.61\mathrm{kN}$ at the free end ($z = l = 150\,\mathrm{cm}$) and to a settlement of the first internal support by $\eta = 15\,\mathrm{mm}$. Three cracks are assumed at the position of supports, having the same depth $d = 2\,\mathrm{cm}$, and hence the same elastic stiffness $K = 1107.42\,\mathrm{kNm}$ of the equivalent discrete spring, as evaluated through Eq. (45). With respect to the previous case, two main differences arise. First, the dimen-

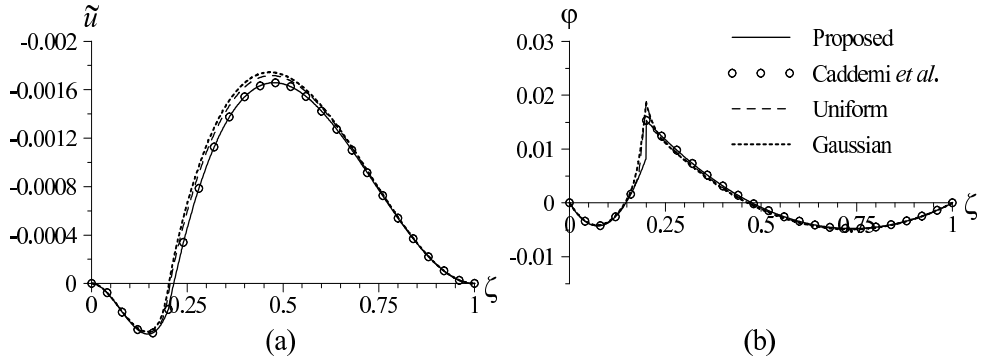

Figure 8: Displacements (a) and rotations (b) of the cracked beam of example 1.

Table 1: Numerical results for example 1

	Proposed ≡ Caddemi *et al.*	Nascent Uniform	Nascent Gaussian	FEM (SAP2000)
$\widetilde{u}(\zeta = 0.5)$	-0.001648	-0.001700	-0.001723	-0.001648
$\varphi(\zeta = 0.75)$	0.004740	0.004836	0.004874	0.04740
$\widetilde{M}(\zeta = 0)$	-0.1160	-0.1149	-0.1142	-0.1160
$\widetilde{M}\left(\zeta = \bar{\zeta}_1^+\right)$	-0.07458	-0.07364	-0.07302	-0.07412
$\widetilde{M}\left(\zeta = \bar{\zeta}_1^-\right)$	0.1997	0.2006	0.2013	0.1944
$\widetilde{M}(\zeta = 1)$	0.03628	0.03656	0.03663	0.03628

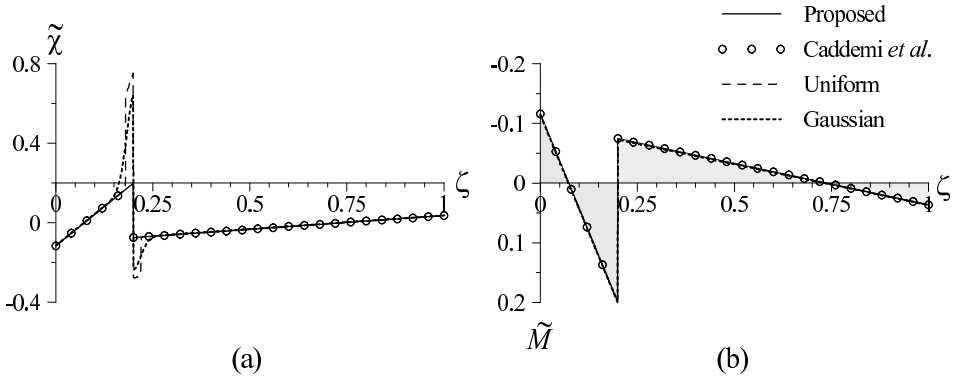

Figure 9: Curvature (a) and bending moment (b) of the cracked beam of example 1.

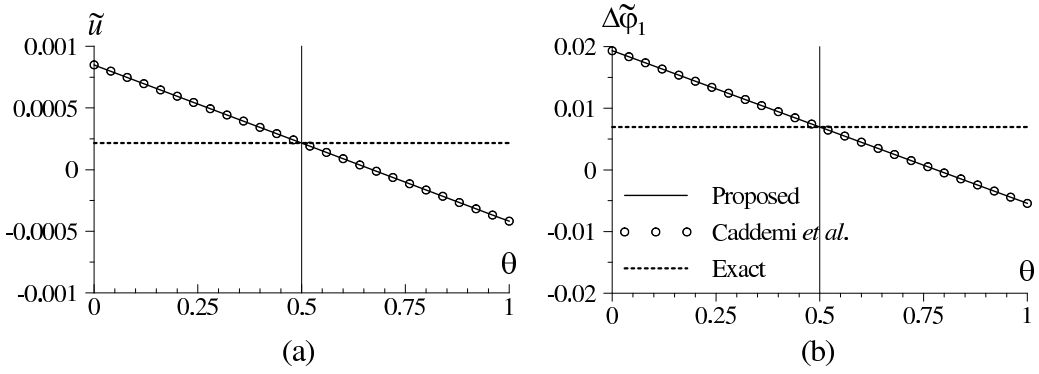

Figure 10: Deflection and rotation's finite jump at the position of the crack in example 1 as a function of the value of Heaviside' unit step function at zero.

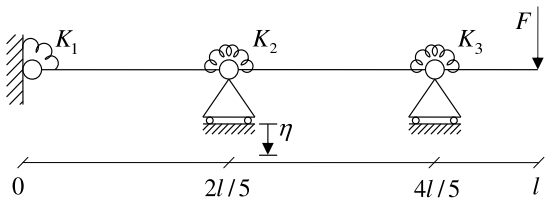

Figure 11: Sketch of the multi-cracked Euler-Bernoulli beam considered in example 2.

sionless load $\widetilde{q}(\zeta)$ acting on the beam is given by the reactions of the intermediate supports:

$$\widetilde{q}(\zeta) = -R_1\,\delta(\zeta - \bar{\zeta}_2) - R_2\,\delta(\zeta - \bar{\zeta}_3)\,, \tag{46}$$

being $\bar{\zeta}_2 = 0.4$ and $\bar{\zeta}_3 = 0.8$ the dimensionless abscissas of second and third cracks (whose positions coincide with those of the internal supports), while R_1 and R_2 are unknown dimensionless forces, which require the support conditions, $\widetilde{u}(\bar{\zeta}_2) = \eta/l$ and $\widetilde{u}(\bar{\zeta}_3) = 0$, in addition to the boundary conditions at $\zeta = 0$ and $\zeta = 1$. Second, since the first crack occurs at the left-hand side extreme of the beam, it follows that the associated increase in the beam flexibility must be imposed just in the right-hand side of the crack. This consideration justifies for the first crack a value of the damage index (α_1) twice that one given by Eq. (23); that is: $\alpha_1 = 0.1316$, while $\alpha_2 = \alpha_3 = 0.0658 = \alpha_1/2$. Importantly, this example demonstrates how the physical soundness of the proposed approach enables one to easily handle particular cases such as a crack at one of the boundaries of the beam. Bending flexibility and bending rigidity of the beam so obtained are depicted in Fig. 12, where the dimensionless standard deviation of nascent deltas $\delta^{(\mathrm{G})}_{\tilde{\sigma}}(\zeta)$ is $\tilde{\sigma} = 0.02$. The validity of the proposed representation of the crack at the fixed end (which may also simulate a partial fixity imposed by an imperfect restraint) is confirmed by the excellent agreement between the results delivered by proposed flexibility modelling and FEM analysis with SAP2000, listed in Tab. 2 for some relevant locations. Very good are also the results obtained by using Gaussian PDFs as nascent deltas instead of Dirac's deltas, as confirmed by Fig. 13, which shows in dimensionless form deflection $\widetilde{u}$, and slope φ along the beam.

Significant discrepancies are observed just at the free end of the beam ($\zeta = 1$), due to a relatively large value of the standard deviation ($\tilde{\sigma} = 0.02$) adopted for the Gaussian nascent deltas. The convergence study reported in the log-log chart of Fig. 14 shows that, as expected, these discrepancies reduce monotonically with the standard deviation $\tilde{\sigma}$.

6.3. Propped short beam with single crack

The final numerical application is devoted to the short beam depicted in Fig. 15, which is clamped at $z = 0$ and supported by a roller at $z = l = 150\,\mathrm{cm}$; a crack of relative depth $d/h = 0.5$ is assumed at midspan position ($\bar{z}_1 = l/2 = 75\,\mathrm{cm}$), and a uniform load of $q_0 = 5\,\mathrm{kN/cm}$ is distributed on the right-hand half of the beam:

$$q(z) = q_0 H\left(z - \frac{l}{2}\right). \tag{47}$$

Since the value of slenderness ration $l/h = 3.33$ is quite small, the Timoshenko beam theory is appropriate. Fig. 16(a) and Fig. 16(b) compare the results in terms of dimensionless deflection $\widetilde{u}(\zeta)$ and sectional rotation $\varphi(\zeta) = \widetilde{\chi}'(\zeta)$, respectively, when Euler-Bernoulli (Eq. (16), dashed lines) and Timoshenko (Eq. (44), solid lines) formulations are adopted. As expected, the Timoshenko beam theory predicts larger deflections and a larger opening of the crack (measured by the finite jump of $\varphi(\zeta)$ at $\zeta = 1/2$), so that the Euler-Bernoulli beam theory would be unconservative. More importantly, the results of the proposed closed-form solution for multi-cracked Timoshenko beams (Eq. (44)) are in perfect agreement with those provided by the FEM code SAP2000: e.g., they both predict deflection at midspan $u = 0.0879\,\mathrm{cm}$ ($\widetilde{u}(0.5) = 0.000586$, downward) and rotation at the position of the roller support $\varphi(1) = 0.00160\,\mathrm{rad}$ (anticlockwise).

7. Concluding remarks

The paper offers a new insight into the linear analysis of multi-cracked beams subjected to static transverse loads. By adopting some common macro-scale simplifications, this study assumes that cracks are always open, i.e. the flexibility due to a localised damage does not change with time, and that their effects can be represented by means of equivalent internal springs with linear moment-rotation constitutive law. Even though apparently straightforward, solutions available in the literature for this problem are not completely satisfactory, either in terms of computational efficiency, when continuity conditions must be enforced with auxiliary equations, or in terms of physical inconsistency, when negative impulses are applied to the flexural rigidity of the beam.

Aimed at overcoming these disadvantages, a novel flexibility modelling has been presented and numerically validated. Unlike the rigidity modelling recently formulated by other investigators (Biondi and Caddemi, 2005, 2007), impulsive terms with meaningful positive sign have been directly introduced in the bending flexibility of the beam at the position of cracks. When actual Dirac's deltas are used, exact solutions are obtained, which are equivalent to those derived by Biondi and Caddemi (2007) for slender Euler-Bernoulli beams. The inadequacy of such analytical solutions in handling situations where bending moment and rotation experience discontinuities at the same abscissa (suggested by Failla and Santini (2007)) has been rebutted with an example (Section 6.1), showing that a proper definition of the Heaviside's unit step function allows catering the exact solution also in this case. The proposed flexibility modelling makes also possible to get approximate solutions when nascent deltas (e.g. uniform and Gaussian probability density functions) are implemented, a feature which is prevented in the rigidity modelling. A closed-form expression has been derived to link the rigidity of internal rotational springs with the corresponding damage coefficients of the proposed approach, which has been further extended to cope with short Timoshenko beams with concentrated losses of flexural stiffness. Numerical results have been presented for selected cases, namely a clamped-clamped slender beam damaged at the

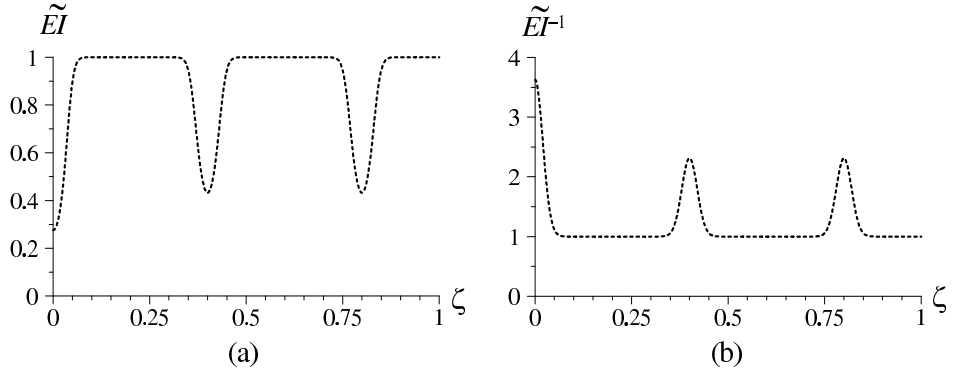

Figure 12: Bending flexibility (a) and rigidity (b) of the multi-cracked beam of example 2 modelled with nascent deltas.

Table 2: Numerical Results for example 2

	Proposed	Nascent Gaussian	FEM (SAP2000)
$\widetilde{u}(\zeta = 1)$	0.002552	0.002003	0.002551
$\varphi(\zeta = 1)$	-0.01943	-0.01714	-0.01942
$\widetilde{M}(\zeta = 0)$	-0.2029	-0.2162	-0.2029
$\widetilde{M}\left(\zeta = \bar{\zeta}_1\right)$	0.2311	0.2412	0.2311
$\widetilde{M}\left(\zeta = \bar{\zeta}_2\right)$	-0.2000	-0.200	-0.2000
$\widetilde{V}\left(0 < \zeta < \bar{\zeta}_1\right)$	1.085	1.143	1.085
$\widetilde{V}\left(\bar{\zeta}_1 < \zeta < \bar{\zeta}_2\right)$	-1.078	-1.103	-1.078

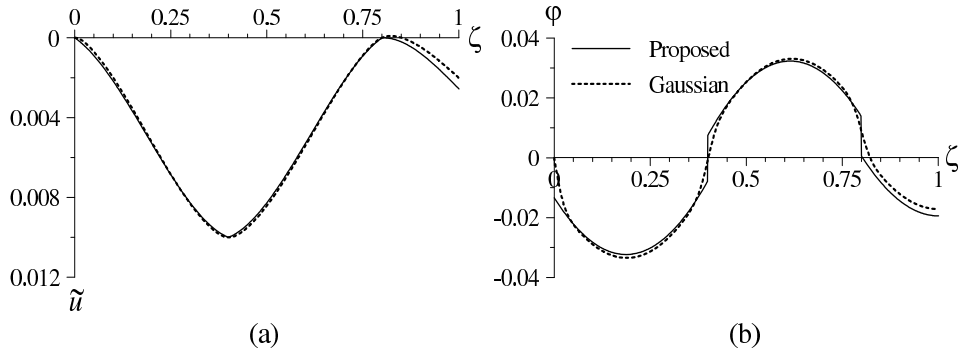

Figure 13: Displacements (a) and rotations (b) of the cracked beam of example 2.

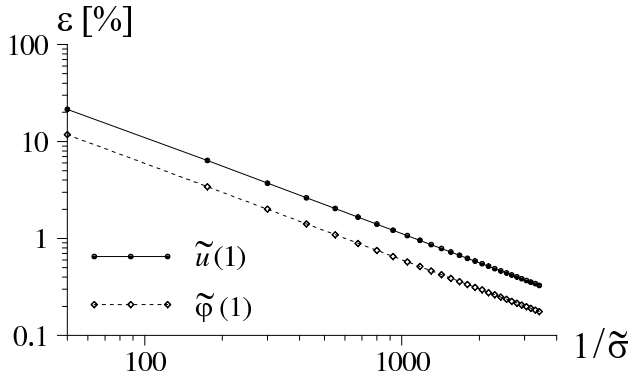

Figure 14: Percentage inaccuracy of the Gaussian model in terms of tip deflection (solid line) and rotation (dashed line) as a function of the measure of the delta's height

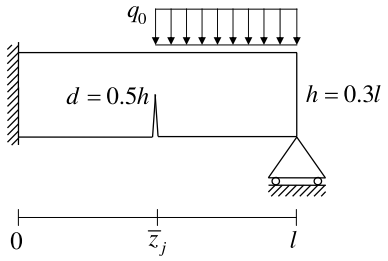

Figure 15: Sketch of the cracked Timoshenko beam considered in example 3.

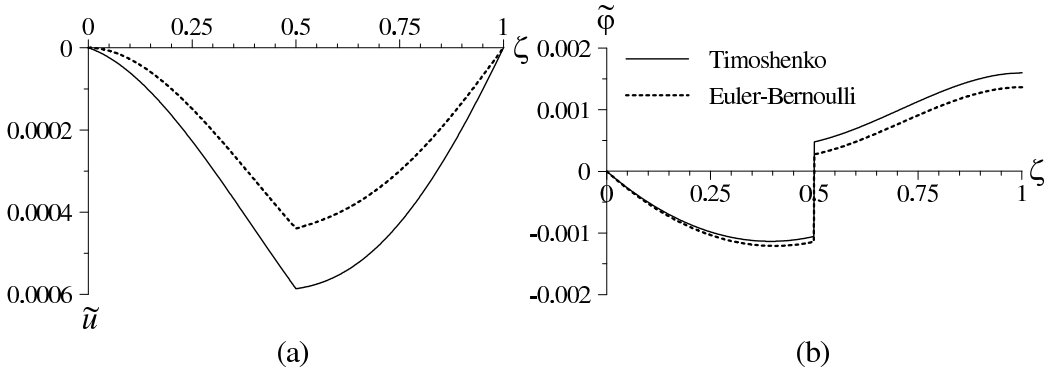

Figure 16: Displacements (a) and rotations (b) of the cracked short beam of example 3.

discontinuity in the bending moment diagram (Section 6.1), a multi-supported beam cracked at the fixed end (Section 6.2), and a short propped beam damaged at midspan (Section 6.3), in so proving the versatility of the proposed flexibility modelling. Building on the results presented in this paper, a further development currently pursued by the authors is the formulations of a consistent two-node finite element for multi-cracked slender/short beam, to be used in the static/dynamic analysis of framed structures. If coupled with crack's initiation and propagation criteria, the proposed approach can be also used to study onset and progressive developments of cracks in slender/short beams, which is another promising extension of the proposed strategy.

References

Bagarello, F., 1995. Multiplication of distribution in one dimension: Possible approaches and applications to function and its derivatives. Journal of Mathematical Analysis and Applications 196, 885–901.

Banan, M.R., Hjelmstad, K.D., 1994. Parameter estimation of structures from static response. i: Computational aspects. Journal of Structural Engineering 120, 3243–3258.

Belytschko, T., Black, T., 1999. Elastic crack growth in finite elements with minimal remeshing. International Journal for Numerical Methods in Engineering 45, 601 – 620.

Bilello, C., 2001. Theoretical and experimental investigation on damaged beams under moving systems. Ph.D. thesis. Università degli Studi di Palermo. Palermo, IT.

Biondi, B., Caddemi, S., 2005. Closed form solutions of Euler-Bernoulli beam with singularities. International Journal of Solids and Structures 42, 3027–3044.

Biondi, B., Caddemi, S., 2007. Euler-Bernoulli beams with multiple singularities in the flexural stiffness. European Journal of Mechanics - A/Solids 26, 789–809.

Brungraber, R., 1965. Singularity functions in the solution of beam-deflections problems. Journal of Engineering Education (Mechanics Division Bulletin) 55, 278–280.

Buda, G., Caddemi, S., 2007. Identification of concentrated damages in Euler-Bernoulli beams under static loads. Journal of Engineering Mechanics 133, 942–956.

Caddemi, S., Calió, I., 2008. Exact closed-form solution for the vibration modes of the EulerBernoulli beam with multiple open cracks. International Journal of Solids and Structures 45, 1332–1351.

Caddemi, S., Calió, I., 2009. Exact solution of the multi-cracked Euler-Bernoulli column. Journal of Sound and Vibration 327, 473–489.

Caddemi, S., Calió, I., M., M., 2010. The non-linear dynamic response of the Euler-Bernoulli beam with an arbitrary number of switching cracks. International Journal of Non-Linear Mechanics 45, 714–726.

Caddemi, S., Di Paola, M., 2008. The Hu-Washizu variational principle for the identification of imperfections in beams. International Journal for Numerical Methods in Engineering 75, 1259–1281.

Caddemi, S., Morassi, A., 2007. Crack detection in elastic beams by static measurements. International Journal of Solids and Structures 44, 5301–5315.

Cerri, M., Vestroni, F., 2000. Detection of damage in beams subjected to diffuse cracking. Journal of Sound and Vibration 234, 259 – 276.

Chondros, T., Dimarogonas, A., Yao, J., 1998. A continuous cracked beam vibration theory. Journal of Sound and Vibration 215, 17–34.

Chondros, T., Dimarogonas, A., Yao, J., 2001. Vibration of a beam with a breathing crack. Journal of Sound and Vibration 239, 57–67.

Cicirello, A., 2007. Risposta esatta di travi con discontinuitá geometriche (in italian). Università degli Studi di Messina - BEng Thesis, Messina, IT.

Dimarogonas, A., 1996. Vibration of cracked structures: a state of the art review. Engineering Fracture Mechanics 55, 831–857.

Failla, G., Santini, A., 2007. On Euler-Bernoulli discontinuous beam solutions via uniform-beam Green's functions. International Journal of Solids and Structures 44, 7666–7687.

Friswell, M., Penny, J., 2002. Crack modeling for structural health monitoring. International Journal of Solids and Structures 1, 139–148.

Hjelmstad, K.D., Shin, S., 1997. Damage detection and assessment of structures from static response. Journal of Engineering Mechanics 123, 568–576.

Irwin, G., 1957. Analysis of stresses and strainsnear the end of a crack traversing a plate. Journal of Applied Mechanics 24, 361–364.

Kelly, J., 2006. Graduate Mathematical Physics. Weinheim: Wiley-VCH.

Kirmsher, P., 1944. The effects of discontinuities on the natural frequency of a beams. Proceedings American Society of Testing and Materials 44, 897–904.

Macaulay, W., 1919. A note on the deflection of beams. Messenger of Mathematics 48, 129.

Moës, N., Dolbow, J., Belytschko, T., 1999. A finite element method for crack growth without remeshing. International Journal for Numerical Methods in Engineering 46, 131 – 150.

Muscolino, G., Palmeri, A., 2005. Maximum resonse statistics of MDoF linear structures excited by non-stationary random processes. Computer Methods in Applied Mechanics and Engineering 194, 1711–1737.

Muscolino, G., Palmeri, A., Sofi, A., 2009. Absolute versus relative formulations of the moving oscillator problem. Computer Methods in Applied Mechanics and Engineering 46, 1085–1094.

Nguyen, V., Rabczuk, T., Bordas, S., Duflot, M., 2008. Meshless methods: A review and computer implementation aspects. Mathematics and Computers in Simulation 79, 763 – 813.

SAP2000, version 14.1.0. CSi: Computers and Structures, Inc. Computer software.

Skrinar, M., 2009. Elastic beam finite element with an arbitrary number of transverse cracks. Finite Elements in Analysis and Design 45, 181 – 189.

Skrinar, M., Pliberšek, T., 2007. New finite element for transversely cracked slender beams subjected to transverse loads. Computational Material Science 39, 250 – 260.

Strichartz, R., 2003. Guide to Distribution Theory and Fourier Transforms. Singapore: World Scientific.

Yavari, A., Sarkani, S., Moyer, E., 2000. On applications of generalized functions to beam bending problems. International Journal of Solids and Structures 37, 5675 –5705.

Yavari, A., Sarkani, S., Reddy, J., 2001. On nonuniform Euler-Bernoulli and Timoshenko beams with jump discontinuities: application of distribution theory. International Journal of Solids and Structures 38, 8389–8406.

Yaw, L., Sukumar, N., Kunnath, S., 2009. Meshfree co-rotational formulation for two-dimensional continua. International Journal for Numerical Methods in Engineering 79, 979 – 1003.